Effect of temperature change on the refractive index of an egg white and yolk: a preliminary study

Patryk Sokołowski*

Department of Metrology and Optoelectronics, Faculty of Electronics, Telecommunications and Informatics, Gdańsk Tech, 11/12 Narutowicza Street, 80-233 Gdańsk, Poland

Received April 01, 2022; accepted June 30, 2022; published June 30, 2022

Abstract—In this article, the refractive index of an egg white and yolk depending on temperature in the range 30–47°C over 1550 nm was determined. The measurement head was constructed as a fiber optic Fabry-Perot interferometer with interference between the polished fiber end-face and the aluminum weighing dish. The measurement setup was made of an optical spectrum analyzer, superluminescent diode with a central wevelength of 1550 nm, 2:1 fiber coupler and heat plate.

European egg consumption amounts to 240 eggs per person, per year [1]. Eggs provide key sources like proteins, fats, vitamins, minerals and bioactive compounds. The composition of eggs and their net amount could be influenced by hens' age and diet, strain and environmental conditions [2]. The refractive index (RI) could be a potential marker of those factors. The RI of biological cells describes their interaction with light and depends on the concentrations of water and nutrients [3]. In biological samples, establishing a minor change in the refractive index is often more important than the absolute value of the index itself.

In this work, Fabry-Perot interferometers (FPI) were used as sensors to determine the refractive index of egg white and yolk. In order to measure the RI of a liquid biological sample like an egg white or yolk, the measurement setup with an FPI sensor as shown in Fig. 1 was configured. FPI was applied as an optical sensor for measurement of physical parameters due to their high resolution, fast response time. Additionally, fiber-optic sensors are biocompatible and can easily be tuned by modifying their design with optical coatings [4].

The measurement setup was made of an optical spectrum analyzer (Ando AQ6319, Yokohama, Japan) as the optical signal processor, a superluminescent diode with a wavelength of 1550 ± 20 nm and spectral width of 35 nm (SLD-1550-13, FiberLabs Inc., Fujimino, Japan), 2:1 fiber coupler (Lightel, Renton, Washington, USA) and a heat plate (own construction).

In a fiber FPI, the phase of the interference signal is linearly proportional to the optical length of the cavity, defined as the product of cavity length and the refractive index of the medium filling the cavity [5].

* E-mail: patsokol@pg.edu.pl

The phase shift can be calculated by [6]:

$$\varphi = \frac{4\pi nL}{\lambda}, \tag{1}$$

where φ – the phase shift, n – the refractive index, L – the geometrical path length, λ – the wavelength.

In the experiment, geometrical path length L is the cavity length, which is the distance between the polished fiber end-face and the refractive surface (an aluminum weighing dish).

Information about the measurement is encoded in the full spectrum of light reflected from the sensing interferometer [7]. The optical spectra of FPI filled with air were measured by the optical spectrum analyzer shown in Fig 2. The distance between the sensor head and the reflective surface in the device influences the visibility of the interferometric fringes, as the light beam diverges and is coupled back into the fiber with differing efficiency [8]. The sensitivity of the measurement depends on visibility.

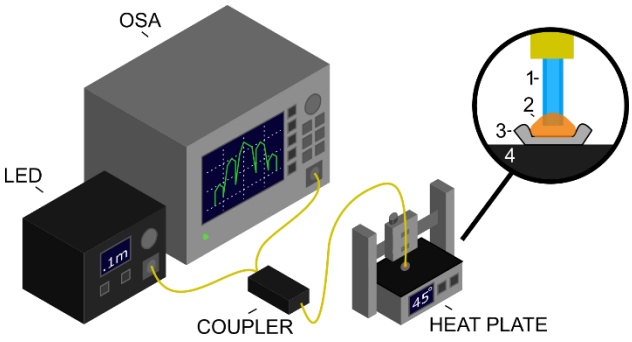

Fig. 1. Measurement setup: (1) fiber, (2) sample, (3) aluminum weighing dish, (4) heat plate.

The measured spectra and cavity length are used to calculate the refractive index of a sample. At first, the estimation of cavity length was conducted by measuring air at room temperature with a built measurement setup using [9]:

$$L * n = \frac{1}{2}\left(\frac{\lambda_1 * \lambda_2}{\lambda_2 - \lambda_1}\right), \quad (2)$$

where λ_1 and λ_2 are the wavelengths of two neighboring maxima near the central wavelength position.

As shown in Fig. 2, λ_1 and λ_2 are the center wavelengths of two adjacent minima in the interference spectrum. The refractive index of air at room temperature is 1.0003 at 1550 nm [9].

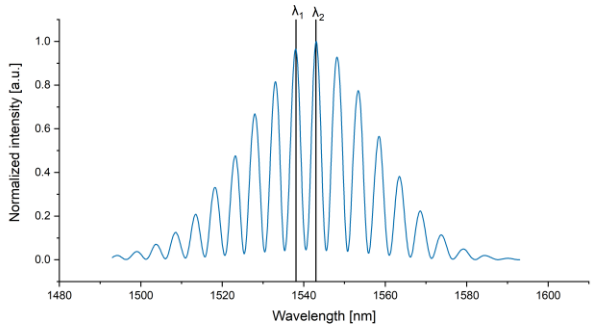

Fig. 2. Spectral signal of cavity filled with air.

During measurements, the cavity length was constant, but changes in the refractive index of the sample in the cavity were impacting optical path length. Equation (2) can be used to calculate either the absolute refractive index n or the geometrical cavity length L. In measurements, the cavity length was set at 238.8 μm for the egg white and 211.7 μm for the egg yolk. Based on the estimated cavity length and the measured sample interference signal, the refractive index was calculated. In Fig. 3, one of the measurement spectra at 35°C was shown. The distance between λ_1 and λ_2 in spectra signals of air and egg differs.

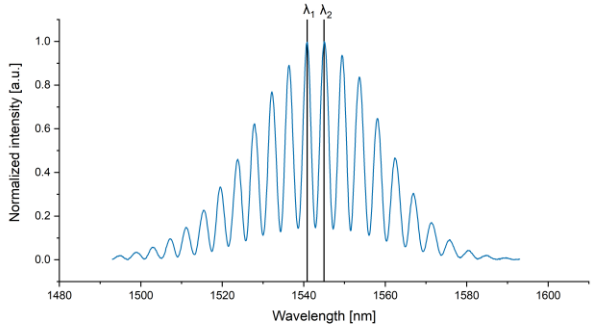

Fig. 3. Spectral signal of egg white at 35°C.

Sample eggs were bought in a supermarket labeled as free-range eggs and the entire box of 6 eggs was measured. The cracked egg was separated to white and yolk, then few milliliters were put on an aluminum weighing dish. Refractive index measurements were performed in a temperature range of 30–47 degrees Celsius, with a step of 1 degree. At each temperature, 6 measurements were performed to determine the median value and to reject measurements that deviate significantly from the other samples' refractive index.

Figures 4a and 4b show the refractive index as a function of temperature. Our measurement focused on the temperature range similar to that of organisms. The refractive index varies between samples, because a different composition of each egg. Boxplot charts were used to show the statistical analysis of the measurement data. The sample represented by the symbol 'o' is an outlier, caused by measurement error. The straight lines inside the boxes indicate a median value based on all measurement series. The distance between the top and bottom edges of the box is the interquartile range (IQR). The dashes indicate minimum and maximum values that were considered as valid. Outlier samples represented by the symbol 'o' are the values that are more than 1.5 IQR away from the box.

The Matlab boxplot algorithm does not always indicate outliners correctly, this can be seen in Fig. 4a. When measured at 46 degrees, the measurements that indicated a value of 1.32 should be counted as outliners. The more measurements that are made, the better the statistics will be and the more erroneous measurements will be detected.

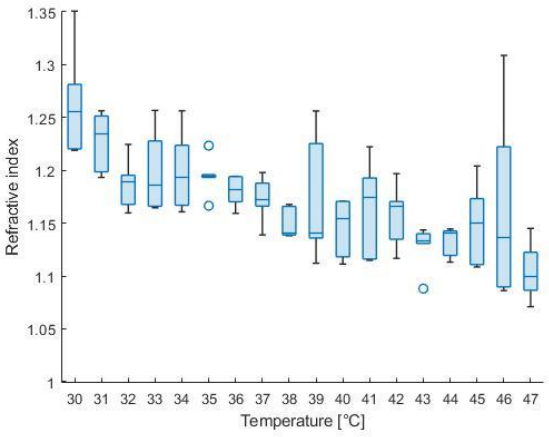

Fig. 4a. Refractive index changes of egg white at 1550 nm.

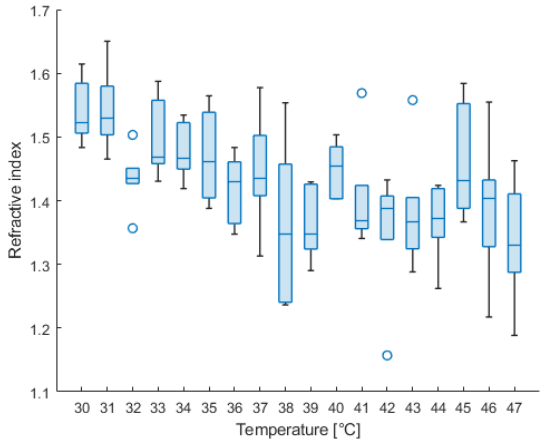

Fig. 4b. Refractive index changes of egg yolk at 1550nm.

Summarizing, the measurement setup allows for determining the refractive index. The obtained results show that refractive index of egg parts strongly depends on temperature and these changes are visible.

This work was supported by the DS programs of the Faculty of Electronics, Telecommunications and Informatics of the Gdańsk University of Technology. The financial support was provided by the DEC-1/2021/IDUB/II.2/Np grant under the NEPTUNIUM Enhancing Baltic Region Research Cooperation (Gdańsk University of Technology) and by the 25/2022/IDUB/III.4.1/Tc grant under the TECHNETIUM Talent Management Grants program, which is herein gratefully acknowledged.

References

[1] P. Magdelaine, "Egg and egg product production and consumption in Europe and the rest of the world, Improving the Safety and Quality of Eggs and Egg Products", Egg Chemistry, Production and Consumption, **3** (2011). https://doi.org/10.1533/9780857093912.1.3

[2] H. Kuang, F. Yang, Y. Zhang, T. Wang, and G. Chen, "The Impact of Egg Nutrient Composition and Its Consumption on Cholesterol Homeostasis", Cholesterol (2018). https://doi.org/10.1155/2018/6303810

[3] J. Gienger, K. Smuda, R. Müller, M. Bär, J. Neukammer, Sci. Rep. **9**, 1 (2019).

[4] P. Listewnik, M. Hirsch, P. Struk, M. Weber, M. Bechelany, M. Jędrzejewska-Szczerska, Nanomaterials **9**, 2 (2019).

[5] Y. Wu, Y. Zhang, J. Wu, P. Yuan, J. Lightwave Technol. **35**, 19 (2017).

[6] M. Islam, M. Mahmood, M Lai, K. Lim, H. Ahmad, Sensors **14**, 4 (2014).

[7] K. Karpienko, M. Wróbel, M. Jędrzejewska-Szczerska, Opt. Eng. **53**, 7 (2014).

[8] M. Kosowska, D. Majchrowicz, K. Sankaran, M. Ficek, K. Haenen, M. Szczerska, Materials **12**, 13 (2019).

[9] G. Xiao, A. Adnet, Z. Zhang, F. Sun, C. Grover, Sensors and Actuators **118**, 2 (2005).

